

# Multimodal Neuroelectric Interface Development

Leonard J. Trejo, Kevin R. Wheeler, Charles C. Jorgensen, Roman Rosipal, Sam T. Clanton,  
Bryan Matthews, Andrew D. Hibbs, Robert Matthews, Michael Krupka

**Abstract**—We are developing electromyographic and electroencephalographic methods, which draw control signals for human-computer interfaces from the human nervous system. We have made progress in four areas: a) real-time pattern recognition algorithms for decoding sequences of forearm muscle activity associated with control gestures, b) signal-processing strategies for computer interfaces using EEG signals, c) a flexible computation framework for neuroelectric interface research, d) non-contact sensors, which measure EMG or EEG signals without resistive contact to the body.

**Index Terms**—Brain-computer interfaces, EEG, EMG, neuroelectric interfaces, electric field sensors.

## I. INTRODUCTION

WE define a system that couples the human nervous system electrically to a computer as a neuroelectric interface: a sensing and processing system that can use signals from the brain or from other parts of the nervous system, such as peripheral nerves, to achieve device control. We regard brain-computer interfaces or BCIs [1] as a subset of neuroelectric interfaces. Our current focus is on using features from electroencephalograms (EEG) and electromyograms (EMG) as control signals for various tasks, such as aircraft or vehicle simulations and other graphic displays.

Our long-term goals are to: a) develop new modes of interaction that cooperate with existing modes such as keyboards or voice, b) augment human-system interaction in wearable, virtual, and immersive systems by increasing bandwidth and quickening the interface, c) enhance situational awareness by providing direct connections between the human nervous system and the systems to be controlled. Our near-term goals include: a) a signal acquisition and processing system for real-time device control, b) automatic EMG-based recognition and tracking of human gestures, c) feasibility testing of EEG-based control methods.

In this paper we will survey selected results and demonstrations of EMG- and EEG-based neuroelectric interfaces. We will describe an EMG-based flight stick, an EMG-based numeric keypad, an EEG-based interface for smooth, continuous control of motion in a graphic display, and comparison of algorithms for modeling the EEG patterns associated with real and imagined hand motion. Finally, we will discuss recent developments of non-contact electric field sensors for EMG and EEG recording.

Our approach is to describe a body of developmental research, which is still in progress, and to indicate methods that have potential for engineering development. Given the BCI focus of this special issue, descriptions of purely EMG-

based interfaces will be brief. We will describe the EEG results and the new sensor developments in more detail.

## II. EMG INTERFACES

### A. EMG-based Flight Stick

In our first demonstration, a computer transformed EMG signals recorded from four bipolar channels placed on the forearm of a subject into control signals for an aircraft simulator. Thus, the processed EMG signals controlled an imaginary flight stick [2]. EMG samples were processed in real time using a flexible signal-processing framework developed in our laboratory. Our feature extraction procedures included routines to filter out redundant and meaningless channels with a mutual information metric [3]. The features were moving averages of the EMG signal from overlapping windows, where the data within a window are nearly stationary.<sup>1</sup> Our model for mapping EMG signal features to gestures uses mixtures of Gaussians within a Hidden Markov Model context. We tested and validated this system with many trials over a two-year period in three subjects, who flew and landed high-fidelity simulations of a Boeing F-15 Eagle or a Boeing 757-200 freighter aircraft. Control of both aircraft was adequate for normal maneuvers. For the 757, a real-time landing sequence under neuroelectric control was filmed at NASA Ames Research Center [on-line demos: [4](#), [5](#)]

### B. EMG-based Numeric Keypad

We have also found that EMG signals from the arm can distinguish typing of one key from another on a “virtual keyboard.” In this demonstration, we programmed a computer to translate eight bipolar EMG signals recorded from the forearm into commands for typing the digits 0-9 on a virtual numeric keypad. We used the same processing system for the typing interface as for the EMG flight stick.<sup>1</sup> However, the Hidden Markov model was retrained using EMG data recorded during typing. Tests were performed with random lists of data to be entered. The typing activity consisted of using the numeric keypad on a computer keyboard. One participant was trained and used for the experiments. He was allowed to type 0 to 9 and “enter.” In tests, the subject typed the series 1 to 9 and 0 three times, or a series of four different dates consisting of four digits each. Using such lists, we found that the digits

<sup>1</sup> We used overlapping moving averages of the rectified, unfiltered EMG signal, sampled at either 500 Hz (joystick task) or 2000 Hz (typing task). The windows contained 128 points and overlapped preceding windows by 96 points. We tried other types of features such as autoregressive coefficients, wavelets, and short-time Fourier transforms, but the moving averages provided the most robust response for everyday use.

0-9 could be detected with 100% accuracy from the processed EMG signals. A demonstration of this system was also recorded at NASA Ames Research Center [on-line demo: 6].

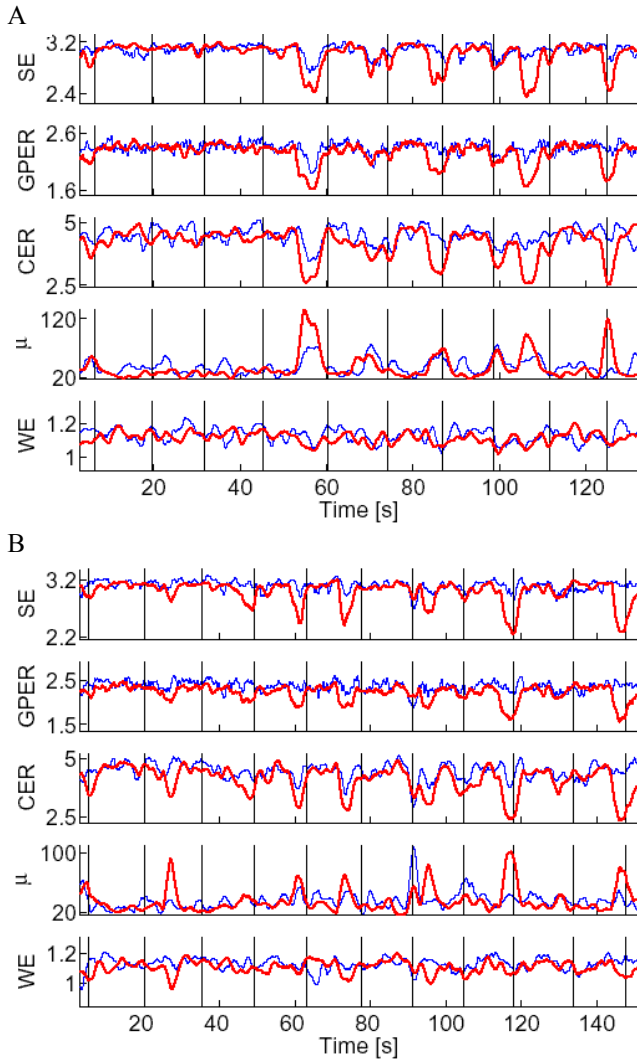


Fig. 1.  $\mu$ -Rhythm filter performance compared with estimates of EEG complexity for the open-loop mouse motion task in Subject 1. Lines show the filter outputs for a series of EEG input windows over time. The heavy line is for SVD component 1, which was derived from earlier 32-channel recordings and estimated here with bipolar electrodes FC1 - TP7. The thin line is for SVD component 2, estimated by AF8 - P4. Vertical lines mark the times when real or imagined hand motions began. Both components change near the onset of real or imagined motions, but component 1 shows larger and more regular changes than component 2. The  $\mu$ -rhythm filter has increased output power, or synchronization, before motions and decreased power, or desynchronization, during or after motions. The other measures (SE, GPER, CER, EW) estimate signal complexity, which change in a direction opposite to that of  $\mu$ -rhythm. For a description of each measure, see the text. A. Real left hand movement. B. Imaginary left hand movement.

### III. EEG INTERFACES

#### A. One-dimensional Graphic Device Control

Previous research has shown that control signals for graphic devices, such as cursors can be drawn from EEG signals such as  $\mu$  and  $\beta$  rhythms [7]. Our approach is to develop a flexible processing system, which will adapt to different tasks and users. To do this we explored several tasks and an array of

pattern recognition and machine learning algorithms.

In *open-loop* tests, we measured EEG during real or imaginary motions and analyzed motion-related changes in the EEG signals later. The tasks were mouse motion and keyboard typing. In *closed-loop* tests we used a real-time system, which provided visual feedback about motion-related EEG signals to the user. The feedback algorithms included narrow-band linear filters for signals such as  $\mu$ -rhythm, broadband filters developed with adaptive linear filters, on-line measures of EEG complexity, and support vector machine classifiers [8-9]. In one closed-loop task, the subject moved a needle gauge up or down by voluntary control of EEG. We trained subjects with a series of target needle positions. In another task, we mapped the subject's EEG signals to left and right turns of a simulation of a Mars rover vehicle as it traveled at constant over a Mars terrain database. In both tasks, subjects viewed either the gauge or the rover on a large video display.

In each task, either 32 or 64 channels of EEG were recorded with a QuickCap (Neuromedical Supplies, Inc.) using the extended International 10-20 System [10] with digitally linked mastoid references (1000 Hz sampling rate, 1 to 30 Hz band pass). We visually inspected the multi-channel EEG recordings and hand-selected artifact-free segments that clearly contained oscillatory activity. On these segments, we used singular value decomposition (SVD) to reduce the multi-channel recordings to a small number of SVD components. Generally, from four to eight SVD components were sufficient to account for 95% of the variance in the hand-selected EEG segments. In some experiments, we approximated these components with a few electrodes, located near the positive and negative extremes of the scalp distributions of the SVD loadings. For these recordings we used either a 2-channel EEG headset (Sensorphone, Allied Products, NY) or disposable self-adhesive Ag-Cl electrodes (Neuromedical Supplies, VA). For example, for the mouse motion task in Subject 1, we approximated the first two SVD components with electrode pairs FC1-TP7 and AF8-P4, respectively. For the mouse motion task in Subject 2, we used a set of 12 electrodes that formed two lines straddling Cz and parallel to the interaural line, with all electrodes uniformly spaced 4 cm apart.<sup>2</sup>

In Subject 1, a 45-year old right-handed male, open-loop tests showed that  $\mu$ -rhythm bursts were visible in the raw EEG. The  $\mu$ -rhythm spectral peak was centered at 9 Hz. A narrow-band 6-11 Hz filter was satisfactory for closed-loop feedback. Using the smoothed filter output power, Subject 1 was able to drive the needle gauge up or down to reach target locations in two testing sessions. In Subject 2, a 32 year-old left-handed male,  $\mu$ -rhythms were not visible in the raw EEG.

Because a filter for  $\mu$ -rhythm was not clearly satisfactory for both subjects, we explored other, more general measures of EEG complexity. The idea here is that regardless of the

<sup>2</sup> In all EEG tests, we ruled out EMG contamination of the EEG signals as source of control. We computed the average event-related band power of several narrow bands between 0.1 and 50 Hz. for both EEG and EMG signals in a 1-s long interval, centered on motion onset. For all bands above 5 Hz, EMG power in the band increased during the motion, whereas EEG power either decreased or remained unchanged.

specific peaks at which sensorimotor EEG rhythms oscillate, their synchrony will influence signal complexity. In our context we define complexity as a measure reflecting changes in EEG regularity or predictability. Signals corresponding to periods of high EEG synchrony will be more regular, predictable, and will have low complexity. Periods of relatively low EEG synchrony will have high complexity.

We examined coarse-grained entropy rates (CER), Gaussian process entropy rates (GPER), spectral entropy (SE) and wavelet entropy (WE). CER is an empirical complexity measure based on stochastic process entropy rates and the Kolmogorov-Sinai entropy of nonlinear dynamical systems [11-12]. CERs have been shown to reflect complexity of physiological signals [10, 13-14]. If we consider the EEG to be a zero-mean stationary Gaussian process we can estimate entropy rates directly from the EEG spectrum [15-16]. Thus we define GPER to be a linear measure, which can fully describe an underlying stationary Gaussian process but cannot describe nonlinear data. SE is a measure which computes Shannon entropy over the normalized power spectral density function; i.e., periodogram [17]. There is a clear connection between GPER and SE as both measures reflect changes of the frequency spectra of the EEG over different brain states. For WE, we extend the concept of SE by replacing the Fourier transform with the discrete wavelet transform [18-19]. So for WE, we computed Shannon entropy over the wavelet coefficients at individual resolution levels.

We applied these measures to open loop data from the mouse motion task in the two subjects. For each measure, estimates were computed for the first two SVD components over time in windows of 2048 samples, which were advanced in 100-sample steps, and further smoothed with a 9-point non-causal running mean (Fig. 1). For Subject 1, three measures, SE, GPER, and CER, reflected changes in EEG synchrony or complexity at nearly the same times as the  $\mu$ -rhythm. The WE measure correlated poorly with  $\mu$ -rhythm. For component 1, the correlation coefficients of each measure with  $\mu$ -rhythm in the real-motion condition were  $r = -.87, -.87, -.87$ , and  $-.62$ , for SE, GPER, CER, and WE, respectively. The corresponding correlations for the imaginary condition were  $r = -.85, -.81, -.79$ , and  $-.55$ . All correlations were significant ( $t$ -test,  $p < .001$ ). Tests of Spearman rank order correlations produced the same results, but with lower values of  $r$  ( $-.49$  to  $-.75$ ). Qualitatively similar results were obtained for Subject 2. We completed several real-time tests and demonstrations of EEG-based control of the Mars rover using complexity measures. For Subject 2, we recorded a demonstration of one of the sessions in which the CER served as the control signal [on-line demo, 20].

### B. EEG-based Typing

For the EEG-based typing tasks we sought to detect the periods of physical keyboard typing activity from EMG-free EEG recordings and to use linear models or machine-learning algorithms to translate the EEG signals into interface commands. We did not seek to identify which keys were pressed. We sought to discriminate typing from rest and also

to discriminate left- from right-hand typing. Our approach was the same as for the motion control tasks: multi-channel EEG recordings were reduced to a few SVD components. These components served as inputs to filters or algorithms that tracked typing behavior. We used the same two subjects who performed the mouse motion tasks and a third subject, a 47-year old right-handed male. Our results are limited to open-loop tests with real motion, and do not imply that classification of EEG is possible without the motor task.

For both subjects, we collected six five-minute runs consisting of typing the keys *A* or *F* with the left pinkie and index fingers, or typing the keys *J* or *;* (semicolon) with the right index and pinkie fingers, or alternating use of the left and right hands within a single run. Typing consisted of self-paced bursts of keystrokes lasting about five seconds followed by about 10 seconds of rest. In other tests, subjects pressed a single key and then rested for about 10 seconds. The EEG was sampled at 1000 Hz, digitally band-passed from 1 to 30 Hz, and re-sampled at 100 Hz. EMG data from the left and right forearms were recorded with four pairs of electrodes placed on the wrists and upper forearms. EMG was sampled at 1000 Hz, digitally band-passed from 30 to 150 Hz, then re-sampled at 300 Hz and rectified. To model typing behavior using EEG, we tested three different types of algorithms:

- *$\mu$ -Rhythm filter*: a linear FIR filter with a pass band centered on the peak of  $\mu$ -rhythm signals observed near electrodes C3 or C4 in the subject's resting EEG.
- *Adaptive linear combiner (ALC)*: the Widrow-Hoff LMS algorithm [21] was used to model periods of the EMG signal corresponding to rest using the EEG time series.
- *Support vector classifier (SVC)*: we used the LIBSVM software for linear support vector classification [22, 23].

We found that the  $\mu$ -rhythm filter was inadequate to model the relationship between EEG and periods of typing or rest. We next explored modeling typing and rest segments with an ALC. Here we found that for Subject 1 a 50-tap ALC was sufficient to track the motion and rest periods associated with typing. For Subject 2, who had no clear  $\mu$ -rhythm, a 500-tap ALC also tracked rest and typing. The results suggest that EEG signals associated with typing can serve as an index of the typing activity. A previous report using a different task drew a similar conclusion [24].

With an ALC, it is possible to freeze adaptation after training and plot the spectrum of the transfer function (Fig. 2). For Subject 1, both the 50-tap and 500-tap filters converged to a set of simple, unimodal transfer functions that favored frequencies below 10 Hz. For subject 2, the transfer functions appeared to be bimodal, with one broad peak in the 5 Hz to 10 Hz range and another broad peak in the 10 Hz to 15 Hz range. In the 500-tap filters for subject 2, a third broad peak is present in the 20 Hz to 25 Hz range.

The ALCs were trained to use EEG-SVD component inputs to model EMG activity exclusively during rest periods. So the ALC output is high during the periods of rest and low during typing. Thus the filter output serves as a rest detector, or conversely, the filter error serves as a motion detector. For Subject 1, the 50-tap filter produced higher output during rest



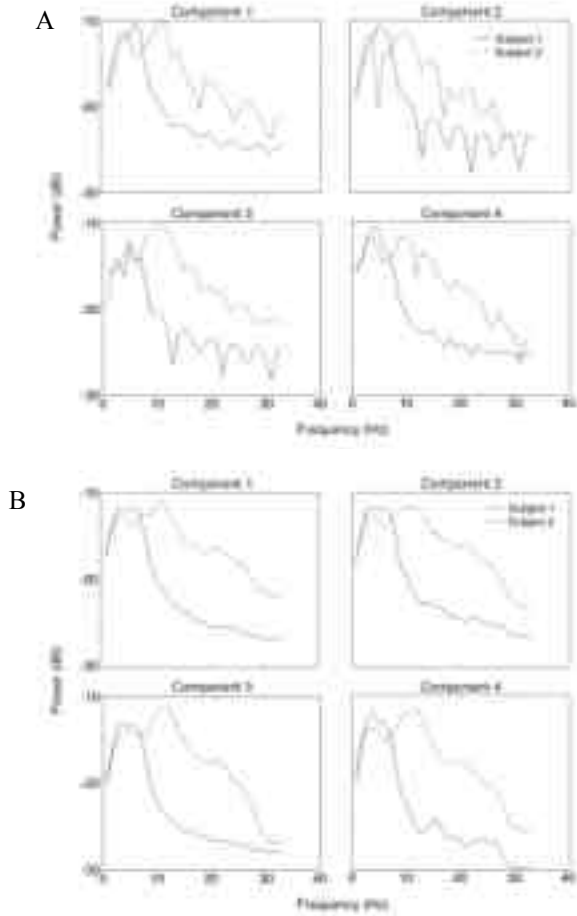


Fig. 2. Transfer functions of the 50-tap (A) and 500-tap (B) ALCs trained to predict rest or right-hand typing periods for the first four SVD EEG components. Typing consisted of bursts of alternating keystrokes using pinkie and index fingers for a few seconds, followed by a few seconds of rest.

than during typing (Fig. 3). For Subject 2 (not shown), the 500-tap filter performed in a similar fashion.

For the conditions in which typing consisted of single keystrokes followed by rest, the ALC filters (and some nonlinear variants) did not serve well for discriminating typing from rest. To solve this problem we attempted to classify EEG segments as either motion or non-motion using windowed EEG signals as inputs to a SVC. Subject 3 performed five 5-minute runs of single-key typing. In each of the first four runs the subject typed for a few seconds using either the left- or right-hand then rested for a few seconds. In the fifth run, the subject alternated between right- and left-hand typing with rest periods in between. Filtered, 64-channel EEG signals served as inputs to the SVC. The data were digitally low-pass filtered at 30 Hz and down sampled to 128 Hz. Successive 128-point segments (1 second of data, with 75% overlap) were labeled as non-motion, left-hand motion, or right-hand motion. Periods were classified as motion when the mean of the corresponding left- or right-hand EMG signal was greater than a predefined threshold. A linear SVC was trained on EEG signals from either the odd- or even-numbered runs and tested on the remaining runs. SVC results for left- vs. right hand typing were inconclusive, with accuracies near 60%. However, the SVCs successfully classified motion vs.

non-motion with accuracies between 78% and 91%. In the most general case -- training with all four initial runs and testing with the final run of mixed hand motion -- the classification accuracies for rest vs. left-hand typing, rest vs. right-hand typing, or rest vs. either hand typing were 85%, 82%, and 88%, respectively. Increasing the EEG bandwidth by re-filtering with a 64 Hz cutoff did not substantially change these values (respectively: 84%, 87%, and 87%), suggesting that EMG artifact did not contribute to the classification.

We also analyzed the weights derived using linear SVC as we did for the ALCs. A spectral analysis of the support vector weights revealed a prominent peak at 18 Hz, which was well defined over centro-parietal electrodes C1, C2, Cp1, and Cp2. We found in a separate analysis that reducing the 64-channels to six channels, including these four, F1 and F2 allowed for classification accuracy of 90% for the test in which the four initial runs served as training data for the fifth run.

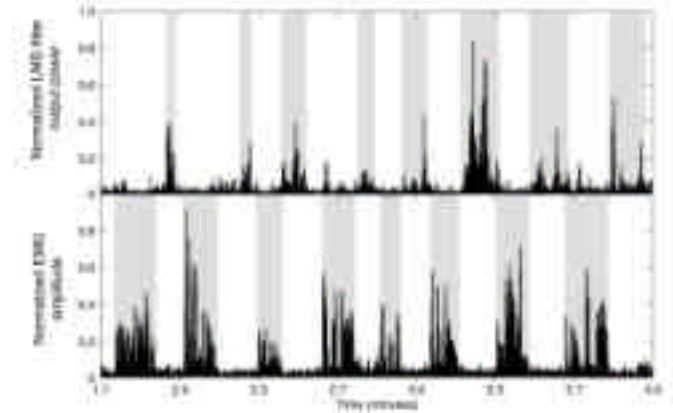


Fig. 3. Performance of the ALC on test data in Subject 1 over time, showing tracking of the motion and rest periods. The upper graph shows the filter output; lower graph shows the rectified EMG time series. Shaded regions correspond to continuous left-hand finger tapping (lower) or rest (upper). Because the filter was trained to model the EEG signals during the rest periods, periods of motion correspond to low filter output power. This is because the EEG signals during motion are different than during rest, and so do not match the filter derived for EEG signals during rest periods.

#### IV. NON-CONTACT SENSOR DEVELOPMENT

NASA Ames Research Center is working with Quantum Applied Science and Research, Inc. (QUASAR) to develop new sensors for neuroelectric recordings. These sensors can measure the electric potential in free space and so do not require resistive, or even good capacitive coupling to the subject. The principal sensor innovation is providing high input impedance for the electrode that senses the free space potential, while accommodating the input bias current of the amplifier. The input capacitance of present electrometer grade amplifiers is of order 1-3 pF. This allows us to arrange the coupling capacitances of the electrometer to yield a near ideal measurement of the bioelectric potential.

Despite its small size, the new sensor is approximately 100 times better than prior electric potential sensors [25]. At 10 Hz it has comparable sensitivity to conventional resistive contact (dry or wet) electrodes. In the off-body mode the sensor can make an accurate measurement through clothing. The sensor also has a broadband response from 0.01 Hz to 10 kHz,

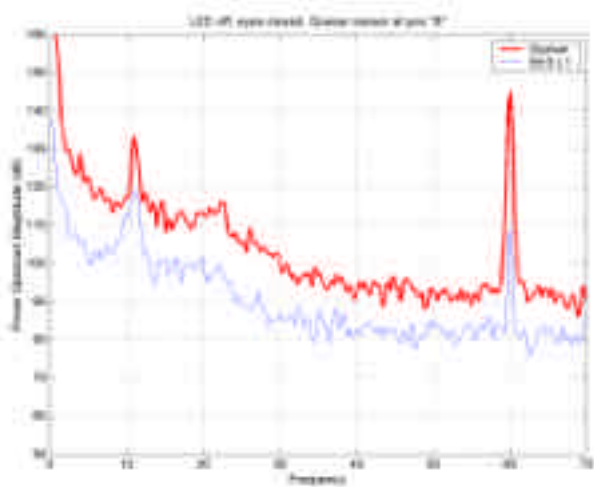


Fig. 4. Power spectrum of recordings from QUASAR and Ag-Cl electrodes in a 21-y old male subject. The Quasar sensor tracks the main features of EEG spectrum seen in the Ag-AgCl electrode recordings. Including the peak near 10 Hz, which reflects endogenous alpha rhythm. The line at 60 Hz is noise from the main power lines resulting from imperfect shielding.

proving sufficient bandwidth to measure EEG and EMG, and essentially all other bioelectric signals of interest.

In our initial tests, we have made direct comparisons between surface recordings of EMG and EEG with non-contact recordings of the same signals.

#### A. EMG Tests.

We recorded EMG from 2 surface Ag-AgCl electrodes spaced 2 cm apart on the forearm over the flexor carpi radialis. The subject was asked to make a fist and this signal was recorded for multiple trials. Then these wet electrodes were removed and replaced by a QUASAR non-contact E-field sensor and the subject repeated the fist clenching exercise. The non-contact sensor recordings tracked the conductive electrode EMG recordings well in the range from 500 Hz to 2000 Hz.

#### B. EEG Tests.

We recorded EEG from 8 surface Ag-AgCl electrodes spaced 4 cm apart and lying on lines 2 cm anterior or posterior to Cz, running from left to right, all referred to average mastoids with ground at AFz. A QUASAR non-contact E-field sensor was tested at the points lying in between the EEG electrodes. EEG was recorded with a Neuroscan Nuamp at gain of 19, band pass 0.1 to 300 Hz, and sampling rate of 1000. The Non-contact sensor tracked the main features of the EEG spectrum seen in the Ag-AgCl electrode recordings (Fig. 4). For example both recordings show a clear peak in the spectrum near 10 Hz, which reflects endogenous alpha rhythm.

### V. DISCUSSION

The EMG-based joystick and typing tasks were chosen to replicate something with which computer users are already familiar. These traditional types of interfaces are certainly not suitable for gesture-based systems as they force unnatural and unintuitive movements. Signal processing and machine learning are maturing to a point whereby methods such as hidden Markov models are suitable for ordinary laptops

without special hardware, however the user interfaces are still 2-D mouse based systems. The ultimate trial of our EMG methodology will be to have a system with a more natural gesture command interface. This could then be used to test the performance of EMG-based systems for everyday use by regular users. Once multiple users have been run on multiple tasks we will then be able to form a usability assessment.

Our EEG-based developments show that 1-D control of a graphic device is feasible as a human computer interface. For different subjects different algorithms may be required, such as  $\mu$ -rhythm filters or complexity measures. Our system is programmed to allow rapid switching among these algorithms or parallel use of the algorithms. We have demonstrated control of a needle gauge and a rendition of turning a Mars rover simulator left and right in real time.

We found that the type of task and the qualities of EEG in a subject interact with the signal processing requirements of the interface. In the simplest case, a narrow band-pass filter tracked 1-D continuous motion for a subject with clear  $\mu$ -rhythm. Other, more general measures, such as SE, GPE, and CER tracked continuous motion in a subject who did not have a clear  $\mu$ -rhythm. Our data sample is too limited to allow us to assess the relative discriminative power of the various measures – we can only show that several measures, which use the full EEG spectrum, provide information similar to that given by a  $\mu$ -rhythm filter. Such measures could be useful in a wider range of subjects, especially those who do not have a clear  $\mu$ -rhythm. In the typing tasks, more elaborate filters, such as an ALC or the SVC-derived filters were required. As the complexity of the task increased from 1-D motion to typing with different fingers on right and left hands, we found that increasing amounts of data and algorithmic complexity were required. For the single-key typing task, as many as 8192 coefficients (64 channels by 128 samples) were used in the SVC. However, we also found that analysis of the SVC weights could reduce the number of channels from 64 to six (or 768 coefficients) without sacrificing accuracy. In any case, the computational demands for using these algorithms in real-time are modest and do not pose a barrier to applications.

At least two serious limitations apply to our data. First, the number of subjects is small. This was necessary to allow us time to explore a wide range of algorithms. Second, our experiments are qualitative and lack statistical and quantitative metrics, such as bit rate, as used in other BCI studies. For the present, we must present these results as merely being indicative of promising BCI approaches for device control.

Our initial findings with the QUASAR non-contact sensors show that it is possible to record both EMG and EEG signals of high fidelity without a conductive link to the body. The bandwidth and gain of these sensors are appropriate for practical applications.

#### ACKNOWLEDGMENT

Charles Curry and Mark Allen of QSS Group, Inc. helped to program the software for the demonstrations. We appreciate the helpful comments of two anonymous reviewers.

## REFERENCES

- [1] Wolpaw JR, Birbaumer N, Heetderks WJ, McFarland DJ, Peckham PH, Schalk G, Donchin E, Quatrano LA, Robinson CJ, Vaughan TM. Brain-computer interface technology: a review of the first international meeting. *IEEE Trans Rehab Engin* 8:164-173, 2000.
- [2] Jorgensen, C., Wheeler, K., & Stepniowski, S. (2000). Bioelectric control of a 757 class high fidelity aircraft simulation. Proceedings of the World Automation Congress, June 11-16, Wailea, Maui, Hawaii.
- [3] Bilmes, J. (1998, April) Maximum mutual information based reduction strategies for cross-correlation based joint distributional modeling. *Proc. ICASSP*, Seattle, 469-472.
- [4] ABC News.com (2001). Twitching Instead of Clicking. [http://abcnews.go.com/sections/wnt/DailyNews/wnt\\_flighttechnology010513.html](http://abcnews.go.com/sections/wnt/DailyNews/wnt_flighttechnology010513.html)
- [5] Ames News (2001a). Extension of the Human Senses Group. Home Page. <http://ic.arc.nasa.gov/projects/ne/ehs.html>
- [6] Ames News (2001b). Extension of the Human Senses Group. EMG Video. <http://ic.arc.nasa.gov/projects/ne/videos/NECD320x240.3.mov>.
- [7] Wolpaw, J. R., D. J. McFarland, et al. (1991). An EEG-based brain-computer interface for cursor control. *Electroencephalography and Clinical Neurophysiology*, 78, 252-259.
- [8] Schölkopf B, Smola AJ: *Learning with Kernels*. The MIT Press, 2002
- [9] Vapnik, V. (1998). *Statistical Learning Theory*. New York, NY: Wiley.
- [10] Jasper, H. (1958). The ten-twenty electrode system of the international federation. *Electroencephalography and Clinical Neurophysiology*, 43, 397-403.
- [11] Palus, M. (1996). Coarse-grained entropy rates for characterization of complex time series. *Physica D*, 96, 64-77.
- [12] Cover, T.M. & Thomas, J.A. (1991). *Elements of Information Theory*. New York: John Wiley & Sons.
- [13] Palus, M., Komárek V., Hrnčíř Z. & Procházka T. (1999). Is nonlinearity relevant for detecting changes in EEG? *Theory Biosci.*, 118, 179-188.
- [14] Rosipal, R. (2001). Kernel-based regression and objective nonlinear measures to assess brain functioning. PhD thesis, Univ. of Paisley: UK.
- [15] Ihara, S. (1993). *Information theory for continuous systems*. Singapore: World Scientific.
- [16] Palus, M. (1997). On entropy rates of dynamical systems and Gaussian processes. *Physics Letters A*, 227, 301-308.
- [17] Inouye, T., Shinosaki, K., Sakamoto, H., Toi, S., Ukai, S., Iyama, A., Katsuda, Y., & Hirano, M. (1991). Quantification of EEG irregularity by use of the entropy of the power spectrum. *Electroencephalography and Clinical Neurophysiology*, 79, 204-210.
- [18] Blanco, S., Figliola, A., Quiñ Quiroga, R., Rosso, O.A., & Serrano, E. (1998). Time-frequency analysis of electroencephalogram series (III): information transfer function and wavelets packers. *Physical Review E*, 57, 932-940.
- [19] Quiñ Quiroga, R., Rosso, O.A., Basar, E., Schürmann, M. (2001). Wavelet entropy in event-related potentials: a new method shows ordering of EEG oscillations. *Biological Cybernetics*, 84, 291-299.
- [20] IC/NEL/EHS (2002). EHS Group. EEG Quicktime Video. <http://ic.arc.nasa.gov/projects/ne/videos/EHS-RR-MARS-ROVER-060402.MOV>.
- [21] Widrow, B. & Stearns, S. D. (1985). *Adaptive Signal Processing*. Prentice Hall, New Jersey.
- [22] Chang, C.-C., and Lin, C.-J. (2001). Training n-support vector classifiers: Theory and algorithms. *Neural Computation*, 13, 2119-2147.
- [23] Hsu, C.-W. and Lin, C.-J. (2002). A comparison of methods for multi-class support vector machines. *IEEE Transactions on Neural Networks*, 13, 415-425.
- [24] Mima, T., Matsuoka, T., Hallen, M. (2001). Information flow from cortex to muscle in humans. *Clinical Neurophysiology*, 112, 122-126.
- [25] Sentman, D. D. (1995). Schumann Resonances, in *Handbook of Atmospheric Electrodynamics*, (H. Volland, Ed.), CRC Press, Boca Raton, Florida.



**Leonard J. Trejo** was born in Mexico City, Mexico, February 24, 1955. He received a B.S. (1977) degree in psychology from the University of Oregon, and M.S. (1980) and PH. D. (1982) degrees in physiological psychology from the University of California, San Diego. He did postdoctoral studies in visual neuroscience at the University of Washington from 1982 to 1984 and postgraduate studies in neural networks and adaptive signal processing at UCLA in 1987.

He served as a research psychologist for the Navy Personnel R & D Center in San Diego from 1984 to 1994, and as assistant

professor of psychology at the University of Illinois at Urbana-Champaign from 1994 to 1997. Since 1998 he has served as Chief of the Human Information Processing Research Branch and as a scientist in the Computational Sciences Division at NASA Ames Research Center.

Dr. Trejo has published over 50 articles in physiology, neuroscience, and biomedical signal processing. In 1992, he pioneered the use of the discrete wavelet transform to analyze complex spatiotemporal data from brain electromagnetic fields. More recently, he has published original research in the area of automatic feature extraction and classification of time-series data corrupted by noise.

**Kevin R. Wheeler** received his B.S. (1988) and M.S. (1991) in Electrical Engineering from the University of New Hampshire, and his Ph.D. (1996) in Computer Engineering from the University of Cincinnati. Before joining NASA Ames Research Center, he performed machine-learning research at IBM Almaden Research Center. He currently serves as Group Leader for the Extension of the Human Senses Group. He is also involved in Earth science data analysis studies. His interests are primarily in machine learning algorithm development for bioelectric and satellite non-stationary data analysis.



**Charles Jorgensen** (M'73-SM'2002) Dr. Jorgensen received his PhD. in Mathematical Psychology from the University of Colorado Boulder in 1973. He has held academic positions at Carnegie Mellon University and the University of Colorado and has been with NASA Ames Research Center since 1990 where he served as Chief of the Intelligent Systems Technology and Computational Systems Branches. He is currently Chief Scientist of the NASA

Neuroengineering Laboratory. Dr. Jorgensen is the author of over 107 technical publications and the recipient of numerous awards and patents including "Most Innovative Technology Award" from the American Nuclear Society, Engram Award from the Department of Defense, the NASA Outstanding Engineering Achievement Medal in 1995 for new neural network paradigms, NASA Exceptional Achievement medal for work in Aeronautics in 1998, and Exceptional Service Medal for outstanding contributions to neural computing in 2001. His current research interests are in neural network damage adaptive control of high performance air and spacecraft, EMG/EEG human interface technologies, and spiking neuron computing architectures.



Roman Rosipal received the M. Sc. degree from Czech Technical University, Prague, in 1993, the M. Sc. degree from Comenius University, Bratislava, in 1999 and the Ph.D. degree from the University of Paisley, Paisley, in 2001. He is currently a Research Scientist at both the NASA Ames Research Center and at the Slovak Academy of Sciences, Bratislava. His major research interests are in statistical learning theory including support vector machines and kernel-based

learning. More recently, he has also become involved in developing an EEG-based brain computer interfaces.



**Sam T. Clanton** was born in Omaha, Nebraska on March 24, 1978. He has a B.S. in biomedical engineering and computer science from The Johns Hopkins University, Baltimore, MD, 2001. He has worked on projects for NASA at the Johns Hopkins Applied Physics Lab and at NASA Ames Research Center in Moffett Field, CA in the fields of biological signal processing, expert systems, and scientific instrumentation.

**Bryan L. Matthews** was born in Monterey, California on October 17, 1979. He has a B.S. in electrical engineering with a minor in physics from Santa Clara University, Santa Clara, CA, 2002. He has worked on projects for NASA at Ames Research Center in Moffett Field, CA in the field of neuroengineering, which include biological signal processing, and scientific instrumentation.

**Andrew D. Hibbs** received his Ph.D. degree from Cambridge University, Cambridge, UK in 1989. He is currently President and CEO of Quantum Applied Science and Research, Inc., San Diego, CA. He is a solid-state physicist with interests in superconducting devices, advanced electric and

magnetic field sensors, nuclear quadrupole resonance, and associated sensing systems.

**Robert Matthews** received the Ph.D. degree in low noise cryogenic instrumentation from the University of Western Australia, in 1993. He is currently Vice President of Quantum Applied Science and Research, Inc., San Diego CA. He is a low noise Instrumentation Engineer with interests in superconducting devices, advanced electric and magnetic field sensors, bioelectronics, and associated sensing systems.

**Michael Krupka** received the B.S. degree in physics from San Diego State University, graduating first in his class. He is currently a lead scientist at Quantum Applied Science and Research, Inc., San Diego CA. He is an Instrumentation Engineer with interests in superconducting devices, advanced electric and magnetic field sensors, bioelectronics, and associated sensing systems.